Modified DNA Aptamer Immobilization via Cu(I)-Stabilizing Ligand-assisted Azide–Alkyne Cycloaddition for Surface Plasmon Resonance Measurement

Nak-Hyeon Kim,[†] Hoa Thi Le,[‡] YongSuk Yang,[‡] Kyung Min Byun,[†,*] and Tae Woo Kim[‡,*]

[†]*Department of Biomedical Engineering, Kyung Hee University, Gyeonggi-do 449-701, Republic of Korea. *E-mail: kmbyun@khu.ac.kr*
[‡]*Graduate School of East–West Medical Science, Kyung Hee University, Gyeonggi-do 449-701, Republic of Korea. *E-mail: tw1275@khu.ac.kr*
Received June 9, 2015, Accepted July 6, 2015, Published online October 9, 2015

The synthesis and binding integrity of an ErbB2-binding modified DNA aptamer (E2Ap) with 5-naphtyl-2′-deoxyuridine is confirmed by electrospray ionization mass spectrometry and by a ^{32}P dot blotting experiment. E2Ap degradation in a conventional Cu(I)-catalyzed azide–alkyne cycloaddition (CuAAC) condition is efficiently prevented by using tris(3-hydroxypropyltriazolylmethyl)amine (THPTA). The immobilization of E2Ap on a surface plasmon resonance (SPR) chip is performed by azido-functionalization and THPTA-assisted CuAAC reaction. The folding, target binding, regeneration, and nonspecific interaction of E2Ap on the SPR chip are verified by both classical and kinetic titration experiments.

Keywords: Modified DNA aptamer, Surface plasmon resonance, DNA immobilization, Cu(I)-catalyzed azide-alkyne cycloaddition, Stabilizing ligand

Introduction

Aptamers are short single-stranded oligonucleotides, either natural or modified RNA/DNA, that fold into well-defined 3D structures and specifically bind to their targets.[1] They are discovered by an *in vitro* selection procedure, called the systematic evolution of ligands by exponential enrichment (SELEX), but are ultimately chemically synthesized as nucleic acid, and thus have specific advantages when compared with antibodies, including enhanced material stability and ease of chemical modification.[2] Eaton co-workers reported a novel SELEX technique with 5-position-modified dUTP (2′-deoxyuridine 5′-triphosphate) derivatives.[3] It is expected that the hydrophobic nature of modified uracil improves the thermodynamic and kinetic characteristics of modified aptamer (low K_D and slow k_{off}). Based on their slow off-rate modified aptamer, Gold *et al.* developed the aptamer-based multiplexed proteomic technology for biomarker discovery.[4]

Conventional aptamer conjugation generally falls into one of the following three categories: (1) amide bond formation of amine-terminated aptamer, (2) self-assembled monolayer of thiol-terminated aptamer on a gold surface, and (3) noncovalent interactions between biotin-tethered aptamer and streptavidin.[5] While the conventional conjugations have been explored in numerous studies, such methods have their own disadvantages. For example, amide coupling has low coupling efficiency and poor reproducibility,[6] while the biotin–streptavidin system requires expensive materials, such as streptavidin and biotin phosphoramidite. Usually, thiol-modified aptamers are supplied in the protected form with the disulfide linkage intact to minimize the potential for oxidation. To use the free thiol aptamers, the disulfide linkage must be reduced with dithiothreitol.[7] Therefore, new chemical methods should be developed to overcome the limitations of conventional aptamer conjugation chemistry.

Recently, the emergence and adoption of Cu(I)-catalyzed azide–alkyne cycloaddition (CuAAC) reaction have been reported to address biomolecule conjugation involving proteins, nucleic acids, nanoparticles, and cells.[8] The CuAAC reaction is characterized by high yields and mild reaction conditions, and tolerates a broad range of functional groups.[9] Catalytic Cu(I) species is in situ generated by the combination of $CuSO_4$ and ascorbate in bioconjugation chemistry. However, the DNA scission activity of ascorbate in the presence of copper ion was already observed by Chiou in 1983.[10] Hydroxyl-radical-like reactive oxygen species generate Cu(I) under aqueous Cu(II)/ascorbate condition, and the Cu(I) ion triggers oxidative nucleobase modification, resulting in DNA strand scission.[11]

The above problem has been overcome through Cu(I)-stabilizing ligands. In 2005, Chidsey[12] and Rajski[13] used a Cu(I)-stabilizing ligand, tris(benzyltriazolylmethyl)-amine (TBTA)[14] and reported the immobilization and the fluorophore labeling of oligonucleotides without significant loss. Carell[15] and Brown[16] reported that terminal alkyne- or azido-functionalized oligonucleotides were successfully conjugated under Cu(II)/ascorbate conditions using Cu(I)-stabilizing ligands. Furthermore, Finn reported a water-soluble Cu(I)-stabilizing ligand, tris(3-hydroxypropyltriazolylmethyl)amine (THPTA).[17]

The surface plasmon resonance (SPR) biosensor has garnered much attention because it allows label-free, quantitative detection of biomolecular interactions in real time.[18] The SPR technique is based on the coupling between incident light and free electrons in a metal. When the momentum of the incident photon matches that of free electrons, the light energy is completely absorbed and converted into collective free electron oscillations called surface plasmons. Since this coupling condition is dependent on the refractive index of the dielectric medium surrounding the metal surface, one can monitor the binding events of biomolecules by measuring the shift in the resonance angle or wavelength.[19]

Several groups have studied aptamer–protein interactions using SPR.[20] Recently, CuAAC-assisted DNA aptamer immobilizations on gold nanoparticles or diazonium film have also been reported.[21] However, the chemistry of DNA aptamer immobilization via CuAAC reaction and the folding, binding, and regeneration of DNA aptamer on the SPR chip have not yet been fully addressed. In this study, we propose a modified DNA aptamer immobilization using a stabilizing ligand-assisted CuAAC reaction and investigate the binding properties of the SPR aptasensor.

Experimental

Materials and SPR Instrument. E2Ap sequence: 5′-d(NCC NGG CAN GNN CGA NGG AGG CCN NNG ANN ACA GCC CAG A)-3′; dN = Nap-dU (11 Nap-dUs in total 40 mer). The 5′ end of E2Ap was modified with 5′-hexynyl phosphoramidite (Glen Research, PN 10-1908, Sterling, VA, USA) using an automated DNA synthesizer. THPTA was synthesized by following the reported procedure and confirmed by ^{1}H, ^{13}C NMR (S1-1, Supporting Information).[17]

An SR7500DC dual-channel SPR system (Reichert Technologies Life Sciences, Buffalo, NY, USA) based on the Kretschmann configuration was employed in our experiments. This apparatus has two measurement channels equipped with an auto-sampler, a syringe pump, and a temperature controller that can maintain the sensor substrate temperature from 10 to 70 °C. The light source of the SPR system is a laser emitting diode with a wavelength of 780 nm. A sensor chip was produced by sputtering a 47.5-nm-thick gold layer onto a 0.9-mm-thick glass substrate after the evaporation of a 1-nm-thick adhesion layer of chromium. The square (12.5 mm × 12.5 mm) substrate was D263 borosilicate glass (Schott, Inc. GER) with a refractive index of 1.52 at $\lambda = 780$ nm.

Aptamer Immobilization on the SPR Chip

N-Hydroxysuccinimide Activation of Carboxylic Acid. Free carboxylic acid on a gold surface (Reichert plain gold surface sensor chip, PN 13206061, 10% COOH-$(PEG)_6$-alkanethiol/ 90% $(PEG)_3$-alkanethiol self-assembled monolayer) was activated by 1-ethyl-3-(3-dimethylaminopropyl)carbodiimide hydrochloride (EDC·HCl) and *N*-hydroxysuccinimide (NHS). Here, a mixture of 0.4 M EDC·HCl and 0.1 M NHS in 1× PBS was employed (pH 7.4, flow rate: 20 μL/min, 10 min).

Functional Group Conversion from NHS-activated Ester to Azide. NHS-activated ester was coupled with 11-azido-3,6,9-trioxaundecan-1-amine (40 mM in sodium acetate buffer (20 mM, pH 5.5), 20 μL/min, 10 min). The unreacted NHS-activated ester was blocked with ethanolamine (1 M) in 1× PBS (pH 7.4, flow rate: 20 μL/min, 10 min). Both the reference and the sample channels were azido-functionalized.

Aptamer Immobilization by THPTA-assisted CuAAC Reaction. E2Ap, $CuSO_4$/THPTA (1:5 molar ratio), and freshly prepared sodium ascorbate were mixed well in 0.1 M phosphate buffer (pH 7.0) (total amount of aptamer = 1.5 μg, $[Cu(II)]_{final}$ = 1 mM, $[ascorbate]_{final}$ = 5 mM). The click cocktail was then flowed at 20 μL/min for 10 min. After the first click reaction, the same coupling reaction was repeated once more. Only the sample channel was functionalized with E2Ap.

SPR Measurement

Aptamer Folding. The click reaction buffer was exchanged by the folding buffer (pH 7.5, 20 mM HEPES, 50 mM NaCl, 2.5 mM KCl, 2.5 mM $MgCl_2$) and washed (flow rate = 20 μL/min, 10 min). Using a temperature controller, the sensor chip was heated to 70 °C, held at this temperature for 10 min, and then cooled to 25 °C at the rate of −1 °C/min. The folding buffer was exchanged with a binding buffer (folding buffer + 0.05% Tween 20).

ErbB2–Aptamer Binding. After stabilization of the baseline, ErbB2 protein in the binding buffer was injected for SPR measurement (flow rate = 20 μL/min in association phase). After the time duration, the binding buffer without ErbB2 was flowed (flow rate = 20 μL/min in the dissociation phase). Data were collected at 37 °C with regeneration (the classical titration) or without regeneration (the kinetic titration). The SPR response units (RU) from the reference channel (azido-functionalized without E2Ap immobilization) were subtracted from the RU of the sample channel (E2Ap-immobilized) prior to the data analysis. Sensorgrams were generated by plotting the RU as a function of time at each ErbB2 concentration.

Washing and Regeneration. After the measurements, the SPR chip was washed with 1× PBS buffer. For the kinetic titration, the SPR chip was used for the next binding without regeneration. For the classical titration, the SPR chip was washed twice with 50 mM NaOH (flow rate = 30 μL/min, 2 min) and the folding buffer (flow rate = 30 μL/min, 2 min).

Results and Discussion

ErbB2 is a receptor tyrosine-protein kinase, also known as HER2 (from human epidermal growth factor receptor 2) or HER2/neu. The overexpression of ErbB2 is related to the development and progression of certain aggressive types of breast cancer. Thus, ErbB2 is considered a valuable marker for tumor diagnosis in ErbB2-positive breast cancer, and clinical diagnostic approaches have been developed to detect ErbB2.[22]

An ErbB2-binding modified DNA aptamer (E2Ap) was discovered, shortened, and synthesized by Aptamer Sciences Inc. (Pohang, South Korea). E2Ap included 5-[*N*-

(1-naphthylmethyl)carboxamide]-2′-deoxyuridines (Nap-dUs)) instead of thymidines (dTs) (Scheme 1(a)). The log *P* difference ($\Delta\log P = 1.81$) between Nap-dU (+0.97) and dT (−0.84) results from the hydrophobicity of the naphthalene moiety. The introduction of hydrophobic groups to aptamers would improve the binding properties of modified DNA aptamers.

Automated DNA synthesis using dA, dT, dG, and dC phosphoramidites has been well established and customized. However, the synthesis and characterization of modified DNA aptamer with Nap-dU require special attention. E2Ap was synthesized using standard β-cyanoethylphosphoramidite chemistry and purified by an AKTA purifier. The purified portion of the sample was quantified by analytical RP HPLC: the purity was found to be 90% (Supporting Information S1-2). In the negative LC-ESI-MS spectrum, we observed a series of *m/z* peaks from partially deprotonated E2Ap (m/z^{obsd}), which were well matched to the calculated *m/z* pattern (m/z^{cald}) with −9 to −15 charges (Figure 1). The agreement between m/z^{obsd} and m/z^{cald} confirmed that E2Ap was successfully synthesized. It is worth mentioning that RP HPLC and deconvolution of LC-ESI-MS would be a quality control method for modified DNA aptamer synthesis.

Equilibrium dissociation constant (K_D) is necessary to confirm the integrity of the target−aptamer specific binding and would be useful for designing the SPR experiment. We measured a rough K_D between ErbB2 and E2Ap using ^{32}P labeled aptamer dot blotting (Supporting Information S2-1). Because the 5′ end of E2Ap was blocked by hexynyl group, the 3′ end of E2Ap was ^{32}P radioisotope-labeled by [α-^{32}P] cordycepin-5′-triphosphate and terminal deoxynucleotidyl transferase (TdT) (Scheme 1(b)). Constant amounts of ^{32}P-labeled E2Ap were incubated at different ErbB2 concentrations. After the incubation, "protein-sticky" ZORBAX resin was added to the E2Ap/ErbB2 mixture.[23] The E2Ap/ErbB2 complex was filtered on the Durapore membrane, while the unbound E2Ap passed through the membrane (Scheme 1(c); Supporting Information S2-2).[24] Phosphorimage analysis and Langmuir isotherm curve fitting showed that E2Ap was bound to ErbB2 with an affinity of ~ 1 nM (Supporting Information S2-3).

DNAs are damaged under a conventional CuAAC condition (*e.g.*, $CuSO_4$ and ascorbate at ~ mM) as described in Introduction. Thus alternative CuAAC reactions without any DNA degradation are important for DNA aptamer immobilization on the SPR chip. Triazole-based copper ligands are often employed to enhance the rate of reaction and protect Cu(I) from oxidation in the presence of oxygen.[24] Triazole-based copper ligands also suppress DNA degradation under conventional CuAAC reaction conditions. THPTA, a water-soluble triazole-based copper ligand was used in these experiments. We tested the stability of E2Ap under various conditions (Figure 2; Supporting Information, S3). The Cu(II) or ascorbate only condition did not give any detectable DNA cleavage (Figure 2, R2 and R4). However, E2Ap was degraded in the presence of Cu(II) and ascorbate within 1 h (Figure 2, A1). In contrast, Cu(II)/THPTA efficiently protected DNA aptamer degradation over a reaction time of 1 h (Figure 2, B1) or even 20 h (Figure 2, B20). Polyacrylamide gel electrophoresis (PAGE) experiment suggested that a

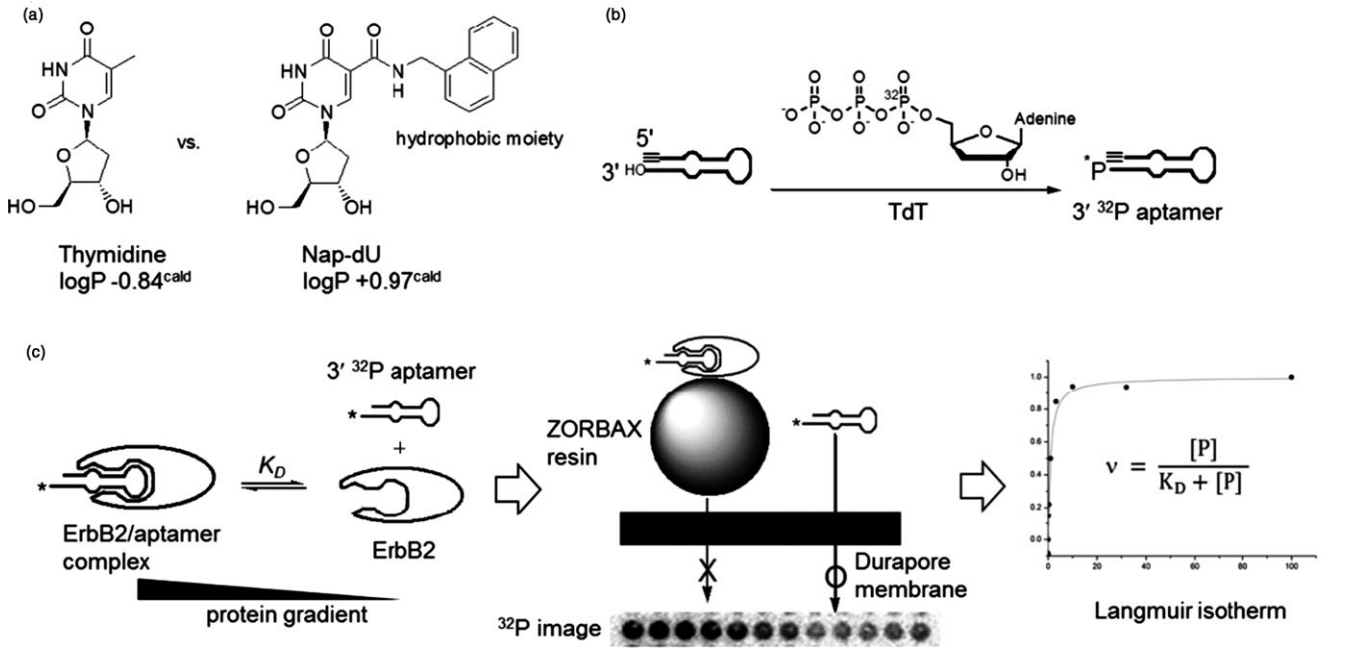

Scheme 1. (a) Molecular structure of thymidine and Nap-dU. The log *P* values were calculated using the Advanced Chemistry Development (ACD/Labs, Toronto, Canada) Software V11.02. (b) ^{32}P radioisotope labeling of DNA aptamer at the 3′ end. Terminal deoxynucleotidyl transferase and [α-^{32}P] cordycepin-5′-triphosphate insert ^{32}P phosphate at the 3′ end of DNA. (c) Workflow diagram of ErbB2/aptamer dissociation constant (K_D) measurement using ZORBAX dot blotting.

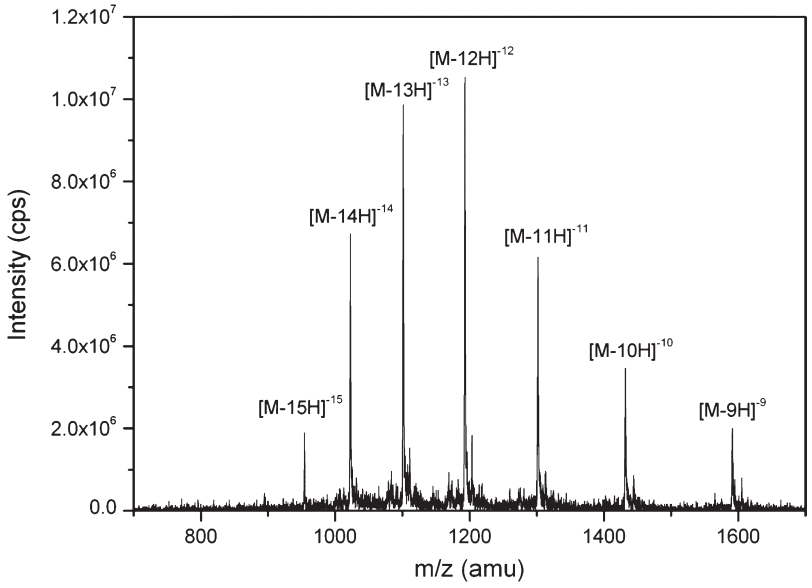

Peak	$[M-15H]^{-15}$	$[M-14H]^{-14}$	$[M-13H]^{-13}$	$[M-12H]^{-12}$	$[M-11H]^{-11}$	$[M-10H]^{-10}$	$[M-9H]^{-9}$
m^{cald}	14307.9	14308.9	14309.9	14311.0	14312.0	14313.0	14314.0
m/z^{cald}	953.9	1022.1	1100.8	1192.6	1301.1	1431.3	1590.4
m/z^{obsd}	954.3	1022.7	1101.3	1192.8	1301.5	1431.9	1591.1

Figure 1. ESI-MS (negative) spectrum of 5′-hexynyl E2Ap with Nap-dU. See SI S1-3 for m^{cald} calculation.

triazole-based stabilizing ligand prevented DNA aptamer degradation in $CuSO_4$ and sodium ascorbate condition.

In order to immobilize E2Ap on the SPR chip, we performed two stepwise reactions: (1) amide formation of NHS-activated ester, and (2) THPTA-assisted CuAAC reaction (Scheme 2). Free carboxylic acids on the gold surface sensor chip (10% COOH-$(PEG)_6$-alkanethiol/90% $(PEG)_3$-alkanethiol self-assembled monolayer on a gold surface) were activated by EDC·HCl and NHS. The NHS-activated surface was coupled with 11-azido-3,6,9-trioxaundecan-1-amine, and then the unreacted NHS-activated ester was blocked with excess ethanolamine (Scheme 2, Step 1). Next, 5′ hexynyl-E2Ap was immobilized on the azido-functionalized SPR chip using $CuSO_4$/THPTA and sodium ascorbate (Scheme 2, Step 2). The sensorgrams of Step 1 and Step 2 are shown in Supporting Information and S4.

The performance of the SPR aptasensors depends on the reliable folding and regeneration of aptamers on SPR chip. The affinity and specificity of aptamers are based on their three-dimensional folding structures. Thus aptamer folding on the SPR chip is crucial to the high specificity and sensitivity of SPR aptasensor. Aptamer regeneration without damage is also important to get reproducible results. We used 70 °C heating for 10 min, and then cooling down to 25 °C at the rate of −1 °C/min for folding and 50 mM NaOH, 30 μL/min, 2 min for regeneration.

All sensor chip surfaces show nonspecific interactions with analytes. Nonspecific interactions should be suppressed so that high specificity and sensitivity could be achieved. A detergent is a good agent to reduce nonspecific interactions. The addition of 0.05% Tween 20 (a nonionic polyoxyethylene surfactant) to a binding buffer (20 mM HEPES (pH 7.5), 50 mM NaCl, 2.5 mM KCl, 2.5 mM $MgCl_2$) efficiently suppressed nonspecific absorption between the E2Ap SPR chip and ErbB2 (Figure 3). The inset of Figure 3 shows that Tween 20 influenced the shape of RU, which is an important factor when determining the precise association rate constant (k_{on}) and dissociation rate constant (k_{off}) in nonlinear curve fitting. In particular, the ΔRU curve obtained without Tween 20 suffered more serious deformation in the higher [ErbB2] region.

The equilibrium dissociation constant (K_D) between the immobilized E2Ap and ErbB2 was measured by both classical and kinetic titration methods. The classical titration of measuring binding constants with affinity-based biosensors involves testing several analyte concentrations over the same ligand surface and regenerating the surface between binding cycles. In contrast, the kinetic titration involves SPR measurement at several protein concentrations without any regeneration steps.[25]

We should know the binding stoichiometry between E2Ap and ErbB2 for K_D calculation. ErbB2 used in our study is a recombinant human ErbB2/Fc (IgG1) chimera protein. As is well known, two Fc domains form a disulfide-linked homodimer.[26] The dimer structure of ErbB2 was confirmed by SDS-PAGE in nonreducing conditions (220–250 kDa) and in reducing condition (125–130 kDa). Two ErbB2 domains hinged on the Fc-Fc dimer would provide a potential aptamer binding site and E2Ap might be anchored in the hollow between two

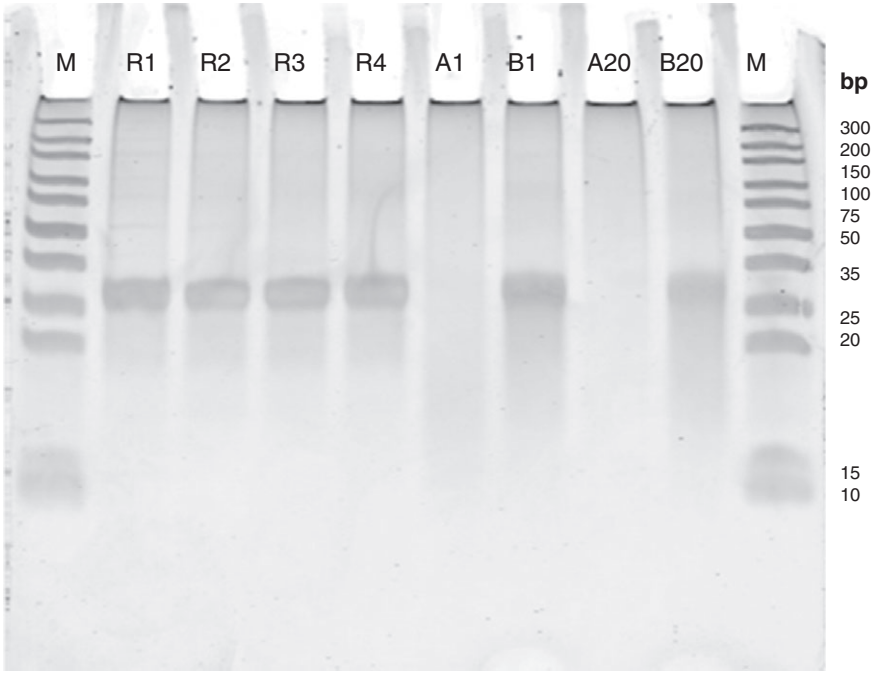

Variation	R1	R2	R3	R4	A1	B1	A20	B20
$CuSO_4$ (mM)	0	1	0	0	1	0	1	0
Cu^{2+}/THPTA (mM)	0	0	1	0	0	1	0	1
NaAsc (mM)	0	0	0	5	5	5	5	5
Reaction time (h)	1	1	1	1	1	1	20	20

Figure 2. Modified DNA aptamer stability under various conditions. M = Fermentas DNA Ladders (GeneRuler Ultra Range DNA Ladder SM1211, ThermoScientific), E2Ap (40 mer) = 10 pmol/μL, reaction buffer = 0.1 M phosphate buffer (pH 7.0), molar ratio of Cu^{2+}/THPTA = 1:5, NaAsc = sodium ascorbate.

ErbB2 domains. Thus we assumed a 1:1 binding mode between E2Ap and ErbB2.

The k_{off}, k_{on}, and K_D values of a range of ErbB2 concentrations were determined by nonlinear curve fitting[23] (Supporting Information S5) or by CLAMP99 data processing using the classical titration (sequential folding/binding/regeneration). The sensorgrams and CLAMP99 fitting curves are shown in Figure 4. The K_D values are 2.1 nM ($k_{off} = 7.0 \times 10^{-4}$ s^{-1}, $k_{on} = 4.0 \times 10^5$ $M^{-1}s^{-1}$) with the curve fitting or 1.3 nM ($k_{off} = 5.5 \times 10^{-4}$ s^{-1}, $k_{on} = 5.0 \times 10^5$ $M^{-1}s^{-1}$) with CLAMP99 (Table 1).

We also determined the k_{off}, k_{on}, and K_D values of a range of ErbB2 concentration using the kinetic titration (sequential binding/washing) (Figure 5). The K_D value by kinetic titration was determined to be 1.3 nM ($k_{off} = 1.2 \times 10^{-4}$ s^{-1}, $k_{on} = 9.4 \times 10^5$ $M^{-1}s^{-1}$). The similar K_D values of two different titration methods (2.1 or 1.3 nM for the classical titration vs. 1.3 nM for the kinetic titration) support that the immobilized E2Ap can be successfully folded and regenerated under the condition used by us.

Actually, RNA cleavage by alkali-promoted phosphodiester transesterification has been well known.[27] DNA is chemically more robust than RNA in high pH. However, the kinetic parameters of DNA stability at a given pH also depend upon other factors such as temperature, divalent cation concentration, or nucleobase composition. In the classical titration, the immobilized E2Ap was washed with a regeneration solution (50 mM NaOH) at each cycle. The k_{off} and k_{on} values at different ErbB2 concentrations showed narrow standard deviations; $k_{off} = 7.0$ $(\pm 4.0) \times 10^{-4}$ s^{-1}, $k_{on} = 4.0$ $(\pm 3.1) \times 10^5$ $M^{-1}s^{-1}$ (Table 1). These reproducible k_{off} and k_{on} values verify that the immobilized E2Ap was not damaged during the folding/regeneration process.

Conclusion

ESI-MS deconvolution and ^{32}P dot blot experiment are good methods to check the synthesis and binding integrity of the modified DNA aptamer. The presence of a water-soluble copper stabilizing ligand (THPTA) enhanced DNA stability in the standard CuAAc condition. We suggested a procedure for DNA aptamer immobilization by a stabilizing ligand-assisted CuAAc reaction and investigated the effects of folding,

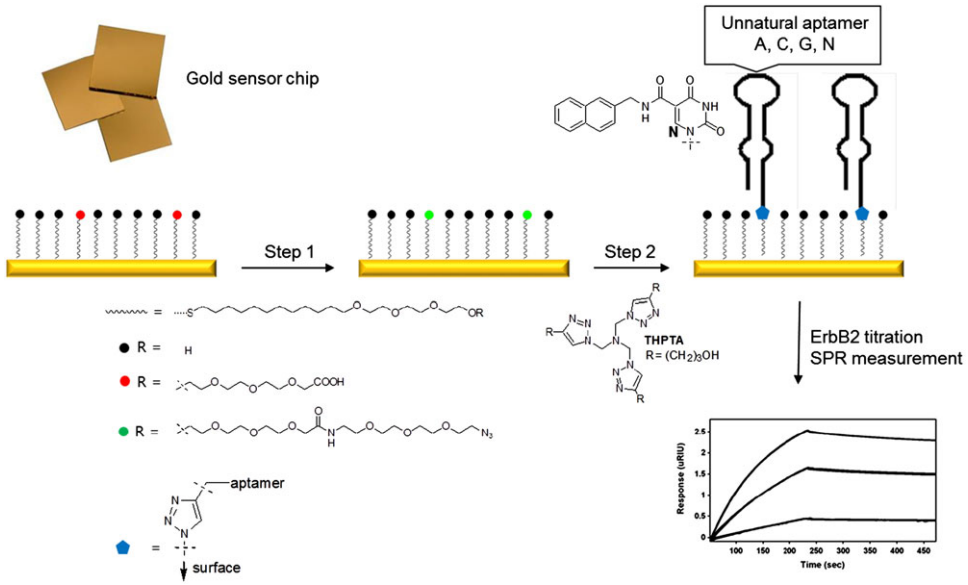

Scheme 2. 5′ Terminal alkyne-modified DNA aptamer immobilization on SPR sensor chip with THPTA-assisted CuAAC reaction. Step 1. -Azido-functionalization, (i) carboxylic acid activation: NHS, EDC·HCl, PBS buffer; (ii) azido-functionalization and blocking: 11-azido-3,6,9-trioxaundecan-1-amine, sodium acetate buffer (pH 5.5), then ethanolamine. Step 2. Aptasensor, (i) 5′ terminal alkyne modified DNA aptamer immobilization: E2Ap, $CuSO_4$/THPTA (1:5 molar ratio), sodium ascorbate, phosphate buffer (pH 7.0); (ii) folding: 70 °C for 10 min, then cooling to 25 °C at 1 °C/min in HEPES buffer (20 mM, pH 7.5).

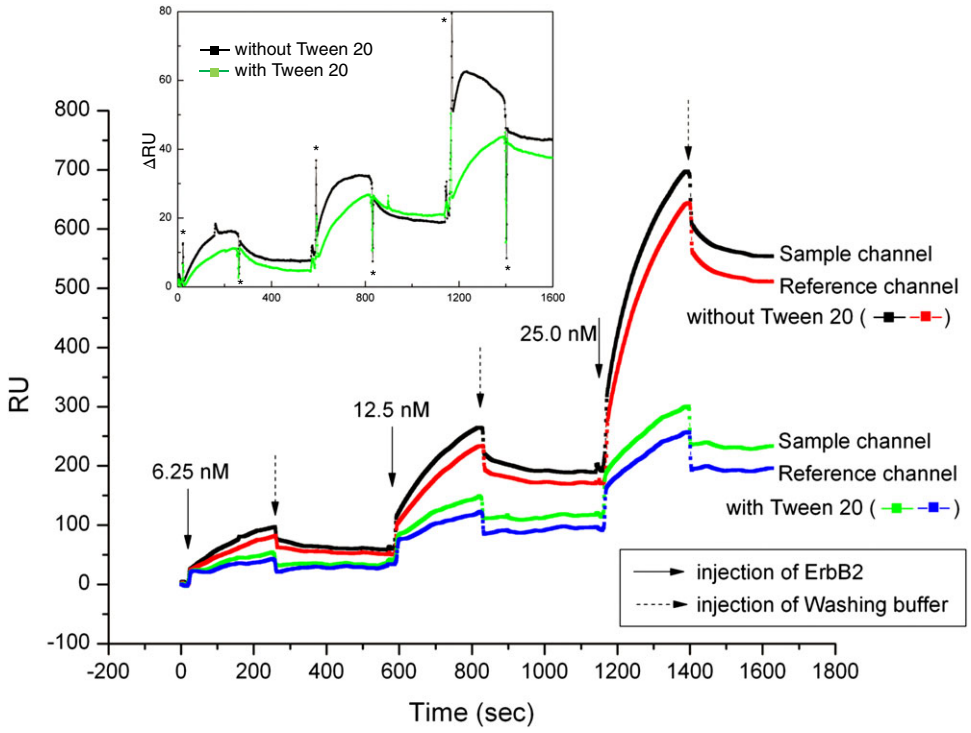

Figure 3. SPR response during three cycles of binding and washing without Tween 20 (black and red squares) and with 0.05% Tween 20 (green and blue squares). Inset: $\Delta RU = RU_{\text{sample channel}} - RU_{\text{reference channel}}$. The spike peaks (*) came from the refractive index perturbations due to binding/washing buffer exchange.

regeneration, and a detergent on protein–aptamer binding using SPR measurements. The reproducible k_{on}, k_{off}, and K_D values in the classical and the kinetic titration methods supported that our folding (70 °C for 10 min, then cooling down to 25 °C at the rate of 1 °C/min) and regeneration (50 mM NaOH) condition were acceptable for SPR measurement

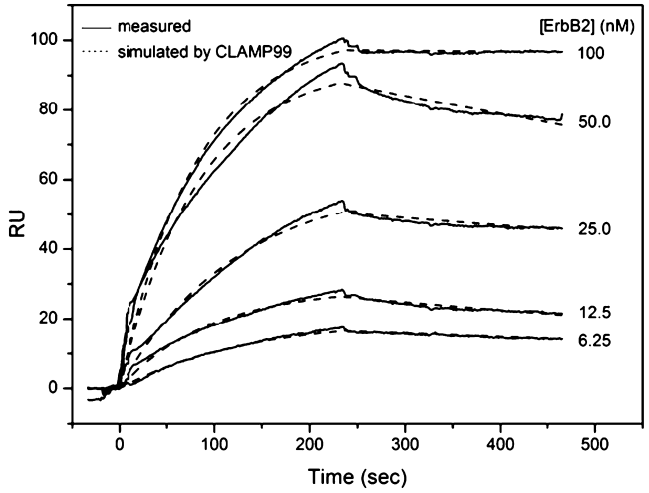

Figure 4. Concentration-dependent SPR sensorgrams by the classical titration method.

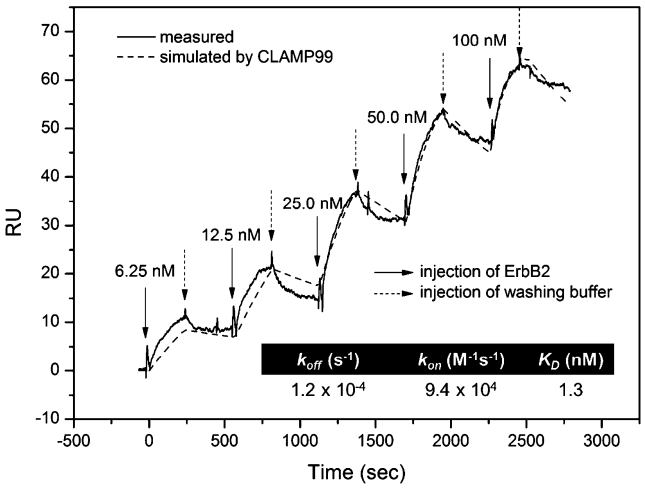

Figure 5. SPR sensorgrams by the kinetic titration method with concentration increase.

Table 1. k_{off}, k_{on}, and K_D values determined by nonlinear curve fitting and CLAMP99 using the classical titration.

	Nonlinear curve fitting			CLAMP99		
[ErbB2] (nM)	k_{off} (s^{-1})	k_{on} (M^{-1} s^{-1})	K_D (nM)	k_{off} (s^{-1})	k_{on} ($M^{-1}s^{-1}$)	K_D (nM)
6.25	6.6×10^{-4}	5.8×10^{-6}	0.9	8.2×10^{5}	1.2×10^{4}	1.5
12.5	1.2×10^{-3}	1.8×10^{-5}	1.5	6.7×10^{5}	1.4×10^{4}	2.2
25	6.2×10^{-4}	1.2×10^{-5}	1.9	2.0×10^{5}	3.8×10^{3}	1.8
50	8.7×10^{-4}	1.6×10^{-5}	1.8	2.1×10^{5}	5.8×10^{3}	2.7
100	1.1×10^{-4}	4.9×10^{-6}	4.3	1.2×10^{5}	1.6×10^{3}	1.3
Average (Standard deviation)	$7.0\ (\pm4.0)\times10^{-4}$	$4.0\ (\pm3.1)\times10^{5}$	2.1 ($\pm$1.4)	$5.5\ (\pm3.4)\times10^{-4}$	$5.0\ (\pm4.1)\times10^{5}$	1.3 ($\pm$0.98)

of the modified DNA aptamer. The addition of 0.05% Tween 20 is a good way to suppress the nonspecific interaction of the aptasensor.

Acknowledgment. This work was supported by a grant from the Kyung Hee University in 2011 (KHU-20110478).

Supporting Information. Additional supporting information is available in the online version of this article.

References

1. M. Blank, M. Blind, *Curr. Opin. Chem. Biol.* **2005**, *9*, 336.
2. A. D. Keefe, S. T. Cload, *Curr. Opin. Chem. Biol.* **2008**, *12*, 448.
3. J. D. Vaught, C. Bock, J. Carter, T. Fitzwater, M. Otis, D. Schneider, J. Rolando, S. Waugh, S. K. Wilcox, B. E. Eaton, *J. Am. Chem. Soc.* **2010**, *132*, 4141.
4. L. Gold, D. Ayers, J. Bertino, C. Bock, A. Bock, E. N. Brody, J. Carter, A. B. Dalby, B. E. Eaton, T. Fitzwater, D. Flather, A. Forbes, T. Foreman, C. Fowler, B. Gawande, M. Goss, M. Gunn, S. Gupta, D. Halladay, J. Heil, J. Heilig, B. Hicke, G. Husar, N. Janjic, T. Jarvis, S. Jennings, E. Katilius, T. R. Keeney, N. Kim, T. H. Koch, S. Kraemer, L. Kroiss, N. Le, D. Levine, W. Lindsey, B. Lollo, W. Mayfield, M. Mehan, R. Mehler, S. K. Nelson, M. Nelson, D. Nieuwlandt, M. Nikrad, U. Ochsner, R. M. Ostroff, M. Otis, T. Parker, S. Pietrasiewicz, D. I. Resnicow, J. Rohloff, G. Sanders, S. Sattin, D. Schneider, B. Singer, M. Stanton, A. Sterkel, A. Stewart, S. Stratford, J. D. Vaught, M. Vrkljan, J. J. Walker, M. Watrobka, S. Waugh, A. Weiss, S. K. Wilcox, A. Wolfson, S. K. Wolk, C. Zhang, D. Zichi, *PLoS One* **2010**, *5*, e15004.
5. S. Balamurugan, A. Obubuafo, S. A. Soper, D. A. Spivak, *Anal. Biochem.* **2008**, *390*, 1009.
6. D. L. Thorek, D. R. Elias, A. Tsourkas, *Mol. Imaging* **2009**, *8*, 221.
7. J. A. Dougan, C. Karlsson, W. E. Smith, D. Graham, *Nucl. Acids Res.* **2007**, *35*, 3668.
8. (a) M. D. Best, *Biochemistry* **2009**, *48*, 6571; (b) E. Lallana, R. Riguera, E. Fernandez-Megia, *Angew. Chem. Int. Ed.* **2011**, *50*, 8794.
9. (a) C. W. Tornoe, C. Christensen, M. Meldal, *J. Org. Chem.* **2002**, *67*, 3057; (b) V. V. Rostovtsev, L. G. Green, V. V. Fokin, K. B. Sharpless, *Angew. Chem. Int. Ed.* **2002**, *41*, 2596.
10. S. H. Chiou, *J. Biochem.* **1983**, *94*, 1259.
11. C. J. Burrows, J. G. Muller, *Chem. Rev.* **1998**, *98*, 1109.
12. N. K. Devaraj, G. P. Miller, W. Ebina, B. Kakaradov, J. P. Collman, E. T. Kool, C. E. Chidsey, *J. Am. Chem. Soc.* **2005**, *127*, 8600.
13. R. L. Weller, S. R. Rajski, *Org. Lett.* **2005**, *7*, 2141.
14. T. R. Chan, R. Hilgraf, K. B. Sharpless, V. V. Fokin, *Org. Lett.* **2004**, *6*, 2853.

15. J. Gierlich, G. A. Burley, P. M. Gramlich, D. M. Hammond, T. Carell, *Org. Lett.* **2006**, *8*, 3639.
16. R. Kumar, A. El-Sagheer, J. Tumpane, P. Lincoln, L. M. Wilhelmsson, T. Brown, *J. Am. Chem. Soc.* **2007**, *129*, 6859.
17. V. Hong, S. I. Presolski, C. Ma, M. G. Finn, *Angew. Chem. Int. Ed.* **2009**, *48*, 9879.
18. J. Homola, *Chem. Rev.* **2008**, *108*, 462.
19. W. K. Jung, N. H. Kim, K. M. Byun, *Appl. Opt.* **2012**, *51*, 4722.
20. (a) P. Subramanian, A. Lesniewski, I. Kaminska, A. Vlandas, A. Vasilescu, J. Niedziolka-Jonsson, E. Pichonat, H. Happy, R. Boukherroub, S. Szunerits, *Biosens. Bioelectron.* **2013**, *50*, 239; (b) D. T. Tran, K. Knez, K. P. Janssen, J. Pollet, D. Spasic, J. Lammertyn, *Biosens. Bioelectron.* **2013**, *43*, 245; (c) J. Ashley, S. F. Li, *Biosens. Bioelectron.* **2013**, *48*, 126.
21. (a) D. Xie, C. Li, L. Shangguan, H. Qi, D. Xue, Q. Gao, C. Zhang, *Sensor. Actuat. B-Chem.* **2014**, *192*, 55; (b) A. Hayat, A. Sassolas, J. Marty, A. Radi, *Talanta* **2013**, *103*, 14.
22. O. K. Mahfoud, T. Y. Rakovich, A. Prina-Mello, D. Movia, F. Alves, Y. Volkov, *RSC Adv.* **2014**, *4*, 3422.
23. M.-E. Han, S. Baek, H.-J. Kim, J. H. Lee, S.-H. Ryu, S.-O. Oh, *Nanoscale Res. Lett.* **2014**, *9*, 104.
24. S. Gupta, M. Hirota, S. M. Waugh, I. Murakami, T. Suzuki, M. Muraguchi, M. Shibamori, Y. Ishikawa, T. C. Jarvis, J. D. Carter, C. Zhang, B. Gawande, M. Vrkljan, N. Janjic, D. J. Schneider, *J. Biol. Chem.* **2014**, *289*, 8706.
25. R. Karlsson, P. S. Katsamba, H. Nordin, E. Pol, D. G. Myszka, *Anal. Biochem.* **2006**, *349*, 136.
26. O. Seifert, A. Plappert, N. Heidel, S. Fellermeier, S. K. Messerschmidt, F. Richer, R. E. Kontermann, *Protein Eng., Des. Sel.* **2012**, *25*, 603.
27. Y. Li, R. R. Breaker, *J. Am. Chem. Soc.* **1999**, *121*, 5364.

